Is gamma-ray burst afterglow emission intrinsically anisotropic?

A. M. Beloborodov, F. Daigne, R. Mochkovitch, Z. L. Uhm

HAL Id: insu-03646059

https://insu.hal.science/insu-03646059

Submitted on 21 Apr 2022

Is gamma-ray burst afterglow emission intrinsically anisotropic?

A. M. Beloborodov,[1,2]★ F. Daigne,[3,4]★ R. Mochkovitch[3]★ and Z. L. Uhm[5]★

[1]*Physics Department and Columbia Astrophysics Laboratory, Columbia University, New York, NY 10027, USA*
[2]*Astrospace Center of Lebedev Physical Institute, Profsojuznaja 84/32, Moscow 117810, Russia*
[3]*Institut d'Astrophysique de Paris, UMR 7095 Université Pierre et Marie Curie-Paris 6 – CNRS, 98 bis, boulevard Arago, Paris 75014, France*
[4]*Institut Universitaire de France*
[5]*Institute for the Early Universe and Research Center of MEMS Space Telescope, Ewha Womans University, Seoul 120-750, South Korea*

ABSTRACT

The curvature of a relativistic blast wave implies that its emission arrives to observers with a spread in time. This effect is believed to wash out fast variability in the light curves of gamma-ray burst (GRB) afterglows. We note that the spreading effect is reduced if emission is anisotropic in the rest frame of the blast wave (i.e. if emission is limb-brightened or limb-darkened). In particular, synchrotron emission is almost certainly anisotropic, and may be strongly anisotropic, depending on details of electron acceleration in the blast wave. Anisotropic afterglows can display fast and strong variability at high frequencies (above the 'fast-cooling' frequency). This may explain the existence of bizarre features in the X-ray afterglows of GRBs, such as sudden drops and flares. We also note that a moderate anisotropy can significantly delay the 'jet break' in the light curve, which makes it harder to detect.

Key words: radiation mechanisms: non-thermal – shock waves – gamma-ray burst: general.

1 INTRODUCTION

Gamma-ray burst (GRB) afterglows are likely produced by relativistic blast waves propagating from the centre of the explosion. This model is, however, challenged by recent observations. In particular, the *Swift* satellite revealed several puzzling features in the X-ray afterglow. It observed an early plateau stage and flares with fast rise and decay times (Burrows et al. 2005; Nousek et al. 2006). Less frequent but even more bizarre are sudden drops in the X-ray light curve (as steep as t^{-10} in GRB 070110; Troja et al. 2007). These behaviours are inconsistent with the standard model of afterglow production.

Can the emission from the forward or reverse shock of the blast wave show strong variations on time-scales $\Delta t \ll t$? It is usually argued that this is impossible: the spherical curvature of the emitting surface (of radius R and Lorentz factor Γ) implies a spread in arrival times of its emission, which washes out variability on time-scales shorter than

$$\tau = \frac{R}{2c\Gamma^2}. \tag{1}$$

For a relativistic blast wave, this duration is comparable to the observed time passed since the beginning of the explosion, $\tau \sim t$. This appears to prohibit any rapid and strong variations in the light curve (see Ioka, Kobayashi & Zhang 2005 for discussion).

Therefore, the observed fast variability in afterglows is usually associated with additional emission from radii much smaller than the blast-wave radius. This model invokes a late activity of the central engine (Zhang et al. 2006). The material ejected at large t and emitting at radii $R \ll \Gamma^2 tc$ will have $\tau \ll t$ and can produce flares with $\Delta t \ll t$. Note however that (i) it is unclear in this model why the observed flares have the approximately universal $\Delta t/t \sim 0.1$ (Chincarini et al. 2007; Lazzati & Perna 2007) and (ii) the very steep drops at the end of some plateaus can hardly be explained by this model unless it assumes that the entire plateau is produced at small radii inside the ejecta and the emission from the blast wave is negligible (Kumar, Narayan & Johnson 2008).

Another difficulty for the GRB theory is that many afterglows lack the predicted 'jet breaks' (Burrows & Racusin 2006; Sato et al. 2007): only a small fraction of afterglow light curves show a clear achromatic break that is expected from jets (Willingale et al. 2007).[1] Some bursts show X-ray light curves extending for tens to hundreds of days with a constant temporal slope (Grupe et al. 2007). The interpretation of these observations is difficult and often leads one to assume large jet opening angles, implying in some cases extremely high energy for the explosion (Schady et al. 2007).

An implicit assumption in the general discussion of these puzzling features is that the emission is isotropic in the rest frame of the relativistically moving source (however see Lyutikov 2006). In this paper, we discuss the effects of a possible anisotropy and suggest

★E-mail: amb@phys.columbia.edu (AMB); daigne@iap.fr (FD); mochko@iap.fr (RM); z.lucas.uhm@gmail.com (ZLU)

---

[1] Many afterglows show chromatic breaks, which occur either in the X-ray or in the optical but not in both bands.

that they can help explain observations. In Section 2, we write down a general formula for the observed flux from a flashing sphere when the emission is anisotropic in the source rest frame. In Section 3, we list the consequences of anisotropy for the curvature effect, the jet break in the afterglow light curve and the size of the radio image of the blast wave. In Section 4, we consider the standard radiative mechanism of afterglows – synchrotron emission – and discuss its anisotropy. The results are summarized in Section 5.

2 LIGHT CURVE FROM A FLASHING SPHERE

Let energy E (measured in the lab frame) be instantaneously emitted by a sphere of radius R, which is expanding with a Lorentz factor Γ and a velocity $\beta = v/c = (1 - \Gamma^{-2})^{1/2}$. Distant observers will see the emitted radiation extend over a range of arrival times t due to the curvature of the emitting surface. The observed light curve $L(t)$ from the flashing sphere can be thought of as a Green function of afterglow emission or 'response function' that describes the curvature effect. It depends on the intrinsic angular distribution of the source intensity. Let θ be the photon angle with respect to the radial direction in the local rest frame of the emitting sphere. The intrinsic (comoving) angular distribution of emission (per unit solid angle) can be described by function $A(\theta)$ normalized by

$$\int A(\theta) \, d\Omega = 4\pi. \tag{2}$$

Isotropic emission in the comoving frame corresponds to $A(\theta) = 1$. The photon angle in the static lab frame Θ is related to θ by

$$\cos \Theta = \frac{\cos \theta + \beta}{1 + \beta \cos \theta}. \tag{3}$$

A distant observer will first see photons emitted along the line of sight with $\theta = \Theta = 0$. Let t_0 be the arrival time of these first photons. Photons received at a later time t come from a larger co-latitude Θ on the emitting sphere, related to t by

$$t - t_0 = \frac{R}{c} (1 - \cos \Theta). \tag{4}$$

A time interval δt corresponds to a ring $\delta \cos \Theta = c \delta t / R$ on the sphere. The true energy emitted by this ring is $\delta E = (1/2) E \, \delta \cos \Theta$. The ring is viewed at angle Θ with respect to its normal, and the observed photons are Doppler-boosted in energy by a factor of $\mathcal{D} = \Gamma^{-1}(1 - \beta \cos \Theta)^{-1}$. The Doppler effect also compresses the solid angle of emission by a factor of $\mathcal{D}^{-2}$. Together with anisotropy $A(\theta)$, the Doppler effect determines the amplification factor for the *apparent* isotropic equivalent of emitted energy,

$$\delta E_{\text{app}} = A(\theta) \, \mathcal{D}^3 \, \frac{\delta E}{\Gamma}. \tag{5}$$

The observed luminosity is $L = \delta E_{\text{app}} / \delta t$, which yields

$$L = \frac{cE}{2R} \frac{A(\theta)}{\Gamma^4 (1 - \beta \cos \Theta)^3}, \tag{6}$$

where θ and Θ are related by equation (3). Substitution of $\cos \Theta(t) = 1 - c(t - t_0)/R$ and $\theta[\Theta(t)]$ gives an explicit expression for the light curve produced by the flashing sphere. These equations simplify in the limit $\Gamma \gg 1$,

$$\cos \theta = \frac{\tau - (t - t_0)}{\tau + (t - t_0)}, \tag{7}$$

$$L = \frac{2E}{\tau} A(\theta) \left(1 + \frac{t - t_0}{\tau} \right)^{-3}, \tag{8}$$

where τ is defined in equation (1).

3 SOME CONSEQUENCES OF ANISOTROPY

An isotropic source, $A(\theta) = 1$, after the Doppler transformation to the static frame emits 75 per cent of the energy within $\Theta_{\text{beam}} = 1/\Gamma$. Let us now consider an anisotropic source, $A(\theta) \neq 1$. We will assume that the anisotropy has a front–back symmetry, $A(\theta) = A(\pi - \theta)$; then the net momentum of emitted photons vanishes in the source frame.

Consider, for instance, 'limb-darkened' emission, which is weak near $\theta = \pi/2$ and strong near $\theta = 0, \pi$. The Doppler transformation to the lab frame strongly amplifies the radiation with $\theta \approx 0$ and weakens radiation with $\theta \approx \pi$. As a result, a bright narrow beam is created, so that 75 per cent of energy is now concentrated within $\Theta_{\text{beam}} = (k\,\Gamma)^{-1}$. Here $k > 1$ is a measure of the enhanced beaming of radiation in the lab frame. The beam $\Theta < \Theta_{\text{beam}}$ is emitted with $\theta < \theta_{\text{beam}}$ in the source frame, and one can show that θ_{beam} is related to k by

$$k \approx \sqrt{\frac{1 + \cos \theta_{\text{beam}}}{1 - \cos \theta_{\text{beam}}}}. \tag{9}$$

The increased beaming in the lab frame ($k > 1$) due to limb darkening in the source frame ($\cos \theta_{\text{beam}} > 0$) has several observational consequences that we list below.

3.1 Curvature effect

The curvature effect is expected to control the observed light curve if the source power suddenly drops. The observed luminosity $L(t)$ responds to the drop with a delay according to equation (8). If the emission is isotropic in the source frame, the delay time-scale is $\tau \sim t$ and the steepest possible decay is $L(t) \propto t^{-\alpha}$ with $\alpha = 3$ (e.g. Kumar & Panaitescu 2000). Since limb darkening of the source implies stronger beaming, $\Theta_{\text{beam}} = (k\Gamma)^{-1}$ instead of Γ^{-1}, most of the energy is radiated on a shorter time-scale, τ/k^2, and the slope α is much steeper.

We will discuss this effect in more detail in Section 4. It turns out that a similar conclusion holds for the opposite, limb-brightened, type of anisotropy, when emission is strong near $\theta = \pi/2$ and weak near $\theta = 0, \pi$.

3.2 Jet break

GRB jets are likely to have a small opening angle $\Theta_{\text{jet}} \ll 1$, which reduces their energy $E_{\text{jet}} \approx (\Theta_{\text{jet}}^2/2)E_{\text{iso}}$ (here E_{iso} is the isotropic equivalent of the jet kinetic energy). A break should be observed in the afterglow light curve at moment t_{jet} when the relativistic beaming angle Θ_{beam} becomes larger than Θ_{jet} (Rhoads 1997), and the value of Θ_{jet} may be inferred from the observed t_{jet}. If the afterglow source is limb-darkened so that $\Theta_{\text{beam}} = (k\Gamma)^{-1}$, the jet-break condition becomes $\Gamma \approx (k\Theta_{\text{jet}})^{-1}$, i.e. effectively Θ_{jet} is replaced by $k\Theta_{\text{jet}}$. The standard light-curve analysis can only give the value of $k\Theta_{\text{jet}}$, which overestimates the true Θ_{jet} by a factor of k. The true E_{jet} for a limb-darkened jet is reduced by a factor of k^{-2} compared with the usual estimate.

Limb darkening also implies a significant delay in t_{jet}. For example, consider a blast wave decelerating in a uniform medium. Its Lorentz factor decreases as $\Gamma \propto t^{-3/8}$. The jet break occurs when $\Gamma \approx (k\Theta_{\text{jet}})^{-1}$, and this moment is delayed by a factor of $k^{8/3}$. The usual expression for t_{jet} then becomes

$$t_{\text{jet}} \approx k^{8/3} \left(\frac{E_{\text{iso},53}}{n} \right)^{1/3} \left(\frac{\Theta_{\text{jet}}}{0.1} \right)^{8/3} \text{d}. \tag{10}$$

Similarly, for a blast wave decelerating in a wind medium, $\Gamma \propto t^{-1/4}$ and hence $t_{\mathrm{jet}} \propto k^4$. Even a moderate anisotropy (e.g. $k = \sqrt{3}$, which corresponds to limb darkening with $\theta_{\mathrm{beam}} \sim 60^{\circ}$ in the source frame) can delay the jet break by a large factor (~ 4.3 in a uniform medium, ~ 9 in wind). This could be enough to not detect the jet break with current observational capabilities as the afterglow is dim at late times and the spectral coverage is incomplete to test achromaticity.

3.3 Apparent size of the radio afterglow source

Very long baseline interferometry observations provided the angular size of the radio image of a few GRB afterglows (Frail 1997; Taylor et al. 2005) which helps constrain the ratio of the blast-wave energy to the density of the environment. The best data have been obtained for GRB 030329 and seem to favour a blast wave in a uniform medium with $E_{\mathrm{jet}}/n \sim (1\text{–}5) \times 10^{51}$ erg cm^3 and $\Theta_{\mathrm{jet}} \sim 0.1$ rad (Pihlström et al. 2007).

The apparent size of the afterglow source is given by (e.g. Oren, Nakar & Piran 2004)

$$R_{\perp} \simeq R\,\Theta, \quad \Theta = \min\left(\Theta_{\mathrm{beam}}; \Theta_{\mathrm{jet}}\right), \tag{11}$$

where R is the radius of the emitting shell. With increased beaming due to limb darkening, $\Theta_{\mathrm{beam}} = (k\Gamma)^{-1}$ and $R_{\perp}$ is reduced by a factor of k^{-1}. For a blast wave in a uniform medium, a derivation similar to that in Oren et al. (2004) gives the relation between the ratio of the true jet energy to the external density and observed $R_{\perp}$, t and t_{jet},

$$\begin{aligned}
\frac{E_{\mathrm{jet}}}{n} \approx{} & 10^{51}\, k^4 \left(\frac{R_{\perp}}{6 \times 10^{16}\,\mathrm{cm}}\right)^6 \\
& \times \begin{cases} t_{\mathrm{jet}}^{3/4} t^{-15/4} & \text{(before jet break)} \\ t^{-3} & \text{(after jet break)} \end{cases}\ \mathrm{erg\,cm}^3.
\end{aligned} \tag{12}$$

One can show that k drops out from the similar relation derived for blast waves in wind media, i.e. in that case limb darkening does not affect the relation.

4 ANISOTROPY OF SYNCHROTRON EMISSION

Afterglow is commonly interpreted as synchrotron emission. Its anisotropy naturally results from a preferred orientation of the magnetic field $\boldsymbol{B}$. Magnetic fields inside GRB jets are generally expected to be transverse to the jet direction, as radial expansion quickly suppresses the longitudinal component. Internal or external shocks can generate magnetic fields only in the shock plane (e.g. Medvedev & Loeb 1999). Thus, in various models of the afterglow production[2] it is reasonable to suppose that the magnetic field in the source is perpendicular to its velocity, $\boldsymbol{B} = \boldsymbol{B}_{\perp}$. In addition, we assume that $\boldsymbol{B}_{\perp}$ is tangled on a scale much smaller than R/Γ, so that a distant observer will see a superposition of emissions from many domains with random orientations of $\boldsymbol{B}_{\perp}$. This assumption is motivated by the low polarization in observed afterglows, typically less than a few per cent (e.g. Covino et al. 1999).

The anisotropy of synchrotron emission may be expected to be moderate if the emitting electrons have an isotropic distribution [see

[2] At present, the origin of afterglow emission is unclear. The standard forward-shock model is in conflict with data, and it is possible that the afterglow is produced by a long-lived reverse shock (Genet, Daigne & Mochkovitch 2007; Uhm & Beloborodov 2007).

e.g. calculations by Granot, Piran & Sari (1999) for three possible geometries of the magnetic field]. Even in this case, anisotropy is present because $\boldsymbol{B}$ is confined to a plane. After averaging over random directions of $\boldsymbol{B}_{\perp}$, one finds the angular distribution of emitted power per electron,

$$\frac{\mathrm{d}P}{\mathrm{d}\Omega} = \frac{P_0}{4\pi}\, A_0(\theta), \quad \text{with}\quad A_0(\theta) = \frac{3}{4}\left(1 + \cos^2\theta\right). \tag{13}$$

Here $P_0 = (\sigma_{\mathrm{T}} c/6\pi)\gamma^2 B^2$ is the power of synchrotron emission per electron and σ_{T} is the Thomson cross-section. The resulting radiation is limb-darkened.

In reality, the electron distribution may not be isotropic: electrons may be preferentially accelerated along or perpendicular to the magnetic field, depending on the acceleration mechanism. For instance, the details of electron acceleration in relativistic shocks remain uncertain, despite significant progress in numerical simulations (e.g. Hededal et al. 2004; Spitkovski 2008; Nishikawa et al. 2009), and other mechanisms are possible. We therefore consider both types of electron anisotropy.

Let α be the pitch angle of an electron with respect to the magnetic field. We will describe the distribution of electron directions by the function $f(\alpha)$, normalized by $\int f(\alpha)\,\mathrm{d}\Omega_{\mathrm{e}} = 4\pi$. Synchrotron emission from each electron is strongly beamed along its velocity, and together the electrons emit radiation with angular distribution,

$$\frac{\mathrm{d}P}{\mathrm{d}\Omega_{\mathrm{e}}} = \frac{3P_0}{8\pi}\, \sin^2\alpha\, f(\alpha). \tag{14}$$

The average power per electron is now given by

$$P = \eta P_0, \quad \eta \equiv \frac{3}{8\pi}\int \sin^2\alpha\, f(\alpha)\,\mathrm{d}\Omega_{\mathrm{e}}. \tag{15}$$

Equation (14) describes the angular distribution relative to the local magnetic field. The angle α between the magnetic field and the observer's line of sight is given by $\cos\alpha = \sin\theta\cos\phi$, where $0 \leq \phi < 2\pi$ depends on the orientation of $\boldsymbol{B} = \boldsymbol{B}_{\perp}$. Using equation (14) and averaging over random directions of $\boldsymbol{B}_{\perp}$, one finds that the synchrotron emission has the following angular distribution:

$$\begin{aligned}
\frac{\mathrm{d}P}{\mathrm{d}\Omega} = \frac{\eta P_0}{4\pi}\, A(\theta), \quad \text{with}\quad A(\theta) ={} & \frac{3}{2\eta}\frac{1}{2\pi}\int_0^{2\pi}\left(1 - \sin^2\theta\cos^2\phi\right) \\
& \times f\left[\arccos(\sin\theta\cos\phi)\right]\,\mathrm{d}\phi.
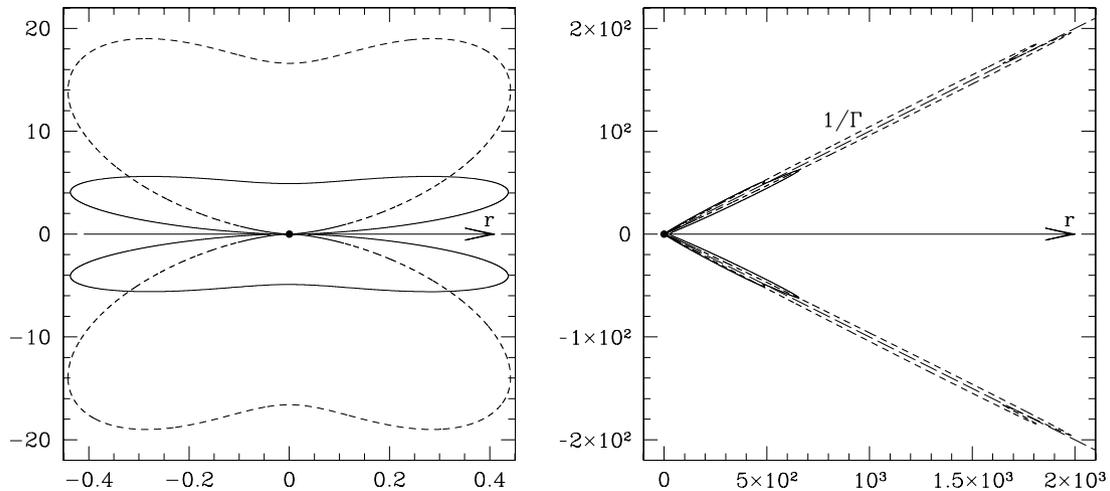\end{aligned} \tag{16}$$

Let us consider two toy models:

$$f_1(\alpha) \propto (a^2 + \sin^2\alpha)^{-3} \quad \text{and}\quad f_2(\alpha) \propto (a^2 + \cos^2\alpha)^{-3}, \tag{17}$$

where a defines a characteristic beaming angle of the electron distribution. These expressions represent two opposite cases where electrons are preferentially accelerated along $\boldsymbol{B}$ (distribution f_1) and perpendicular to $\boldsymbol{B}$ (distribution f_2). Both distributions become isotropic if $a \gg 1$. The opposite limit $a \ll 1$ describes the maximum possible anisotropy: $f_1 \propto \delta(\alpha) + \delta(\alpha - \pi)$ and $f_2 \propto \delta(\alpha - \pi/2)$. By varying the parameter a from ∞ to 0, one can explore the effect of increasing electron anisotropy on synchrotron emission.

The angular distributions $A_1(\theta)$ and $A_2(\theta)$ produced by f_1 and f_2 are shown in Figs 1 and 2. The plot of $A_1(\theta)$ resembles a butterfly with a half-angle $\sim a$ around $\theta = \pi/2$, i.e. the source is limb-brightened. Therefore, the angular distribution of radiation in the fixed lab frame has a sharp peak at $\Theta = \Gamma^{-1}$ when $a \ll 1$. By contrast, $A_2(\theta)$ is concentrated near $\theta = 0, \pi$ with a half-angle $\sim a$; the resulting limb darkening remains, however, finite even if $a \to 0$. In this limit, one finds

$$A_2(\theta) = \frac{2}{\pi\sin\theta} \quad (a \to 0). \tag{18}$$

Figure 1. Diagram of angular distribution of radiation $A_1(\theta)$ (electrons accelerated preferentially along $\boldsymbol{B}$) measured in the source rest frame (left-hand panel) and transformed to the observer frame using $\Gamma = 10$ (right-hand panel). Solid curves correspond to $a = 0.1$ and dashed to $a = 0.03$. Long-dashed lines in the right-hand panel show the cone of opening angle $1/\Gamma$. Rotation of the shown curve about the horizontal axis gives the three-dimensional diagram.
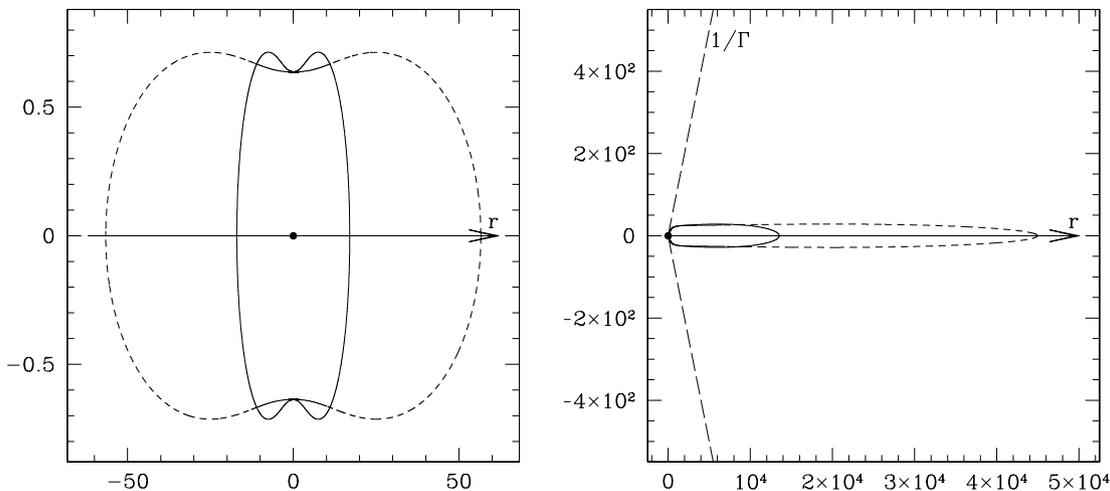
Figure 2. Same as in Fig. 1, but for the angular distribution $A_2(\theta)$ (electrons accelerated preferentially perpendicular to $\boldsymbol{B}$).

The source is weakened at $\theta = \pi/2$ by the modest factor of $2/\pi$ compared with isotropic emission.[3] Also note the difference in the emission power P for the two distributions. For $a \ll 1$, one obtains

$$\eta_1 \approx \frac{3}{2}a^2, \quad \eta_2 \approx \frac{3}{2}. \tag{19}$$
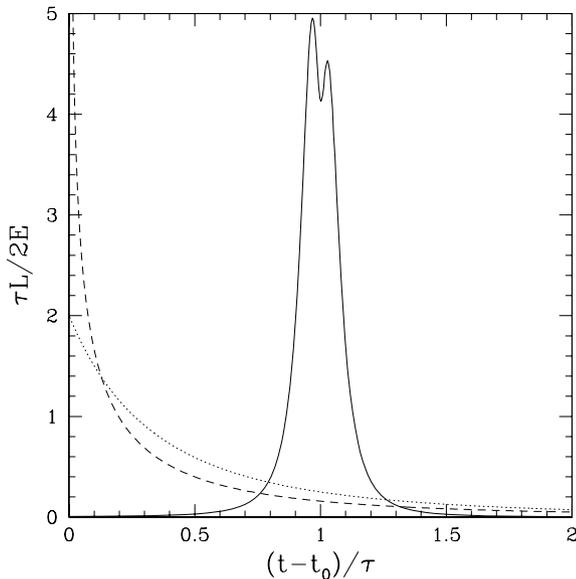
The anisotropy of emission $A(\theta) \neq 1$ can have a strong impact on the afterglow light curves as discussed in Section 3. In particular, the curvature effect, which is described by the light curve from a flashing sphere (the response function, equation 8), is changed. Fig. 3 shows the response function for $A_1(\theta)$ and $A_2(\theta)$ with $a = 0.03$. Compared to the isotropic case, $A(\theta) = 1$, the emitted pulse becomes very narrow if $A(\theta) = A_1(\theta)$, i.e. for the model where electrons are preferentially accelerated along the magnetic field. Photon arrival times then concentrate near a particular $t - t_0 \approx$

---

[3] Electron distribution with $f_2 = \delta(\alpha - \pi/2)$ is a disc in momentum space, with the axis along $\boldsymbol{B}$. After averaging over random orientations of the disc axis in the transverse plane (random directions of $\boldsymbol{B}$) a strong anisotropy is found in $A_2(\theta)$, with a sharp peak in the longitudinal directions $\theta = 0, \pi$. However, a significant 'wing' of emission remains present at large $\theta \sim \pi/2$.

τ (which corresponds to a particular $\Theta = \Gamma^{-1}$) because the limb-brightened radiation is mainly emitted near $\theta = \pi/2$. In the model with angular distribution $A_2(\theta)$ the profile of the response function is steeper than in the isotropic case but can never be as narrow as for $A_1(\theta)$, even in the limit of $a \to 0$.

As a simple illustration, consider a spherical thin shell with constant emission power $\dot{E}_0$, which is moving with $\Gamma_0 = 300$, and suppose that its emission suddenly cuts off at radius $R_{\text{cut}} = 6 \times 10^{16}$ cm. Fig. 4 shows the produced bolometric light curve. It depends on the intrinsic anisotropy of the source, $A(\theta)$. We show three cases: isotropic emission $A(\theta) = 1$, $A_1(\theta)$ and $A_2(\theta)$ (same as in Fig. 3). The limb-brightened emission $A_1(\theta)$ produces a very steep decay in the light curve.

We conclude that extremely fast variations in the light curve, e.g. short flares or steep drops, may be observed in synchrotron afterglows if electrons are preferentially accelerated along $\boldsymbol{B}$, as the response function can be arbitrarily narrow for $a \ll 1$. Note that the emission is limb-brightened in this case, i.e. the situation is opposite to what was considered in Section 3, and the description using $k > 1$ does not apply. Limb brightening has little or no effect on t_{jet} or $R_\perp$, in contrast to the limb-darkened model of Section 3.

Figure 3. Light curve from a flashing sphere with three different angular distributions of emission in the plasma rest frame: isotropic (dotted curve), $A_1(\theta)$ with $a = 0.03$ (solid curve) and $A_2(\theta)$ with $a = 0.03$ (dashed curve). The units for t and L are indicated on the axes ($\tau = R/2\Gamma^2 c$); with these units the area under each curve is unity. The first photon from the flashing sphere reaches the observer at $t = t_0$. The dashed curve has the maximum of about 13 at $t = t_0$.
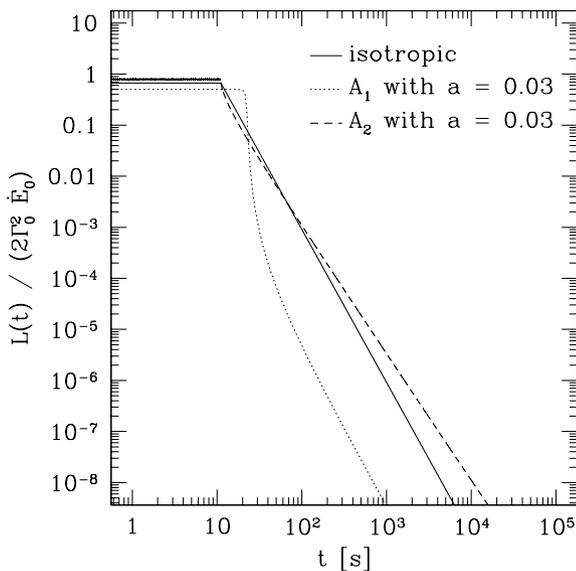
Figure 4. Bolometric light curve from a shell whose emission suddenly cuts off (see the text).

Another implication of the preferential electron acceleration along $\boldsymbol{B}$ is the reduction of synchrotron emissivity by a factor of $\sim a^2$ (cf. η_1 in equation 19). All synchrotron-emission formulae contain only the component of $\boldsymbol{B}$ perpendicular to the electron velocity, which equals $\sim aB$ for $a \ll 1$. Then, the effective ϵ_B that would be inferred from the data using isotropic models will underestimate the real ϵ_B by a factor of $\sim a^{-2}$.

The synchrotron model with angular distribution $A_2(\theta)$ does not predict significant changes in the afterglow light curve, because

limb darkening is never strong for synchrotron emission, regardless of a. A moderate change in t_{jet} and a less pronounced jet break may be expected compared with the case of isotropic emission.

5 DISCUSSION

The usual assumption of isotropic emission in the rest frame of the blast wave is likely to be invalid. Even the standard synchrotron model with isotropic electron distribution produces anisotropic, limb-darkened radiation (Section 4). This fact is a consequence of the preferential orientation of the magnetic field in the blast wave. Strong limb brightening is also possible if the radiating electrons are preferentially accelerated along the magnetic field.

Anisotropy may resolve a few puzzles encountered in the afterglow modelling.

(i) The usual argument that the curvature effect filters out fast variability, prohibiting strong variations in the light curve on time-scales $\Delta t < \tau = R/2\Gamma^2 c$, is not valid for anisotropic emission. An anisotropic variable spherical source can produce fast changes in the light curve, similar to observed bizarre features in GRB afterglows. This result holds for both limb-darkened and limb-brightened types of anisotropy. It suggests that the X-ray flares observed by *Swift* with $\Delta t/t \lesssim 0.1$ do not necessarily imply an additional component of internal origin. Instead they may be produced, for example, by the reverse shock in the blast wave, whose emission may suddenly brighten and weaken as the reverse shock propagates into the inhomogeneous ejecta of the explosion. This model may also explain sudden steep drops in the afterglow light curve as observed in GRB 070110 (Troja et al. 2007). This explanation assumes that the X-ray radiating particles are cooling fast compared with the jet expansion time-scale, as slow cooling would suppress short time-scale variations of the source luminosity.

Examples of such short time-scale behaviours are given by the toy model in Fig. 5. It shows the synchrotron emission produced by a thin shell with Lorentz factor $\Gamma(R) = \Gamma_0 = 300$ at
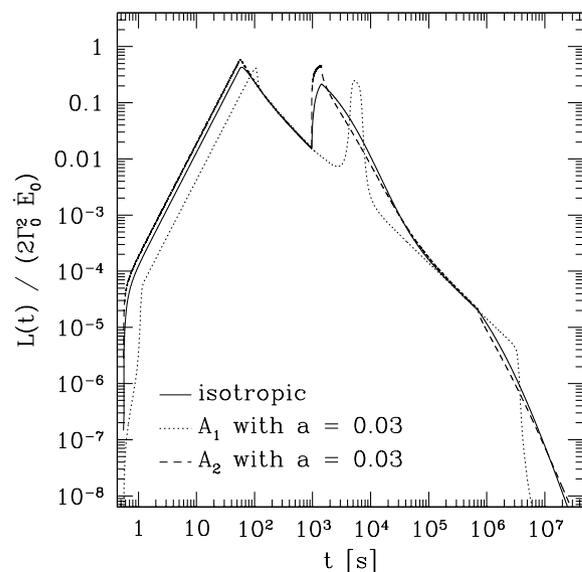
Figure 5. Bolometric light curve for a toy afterglow model (see the text). The result is plotted for three cases: isotropic emission in the rest frame of the blast wave $A(\theta) = 1$ (solid curve), limb-brightened synchrotron emission $A_1(\theta)$ with $a = 0.03$ (dotted curve; see Section 4 for the description of the synchrotron model) and limb-darkened synchrotron emission $A_2(\theta)$ with $a = 0.03$ (dashed curve).

$R < R_{\text{dec}} = 3 \times 10^{17}$ cm and $\Gamma(R) = \Gamma_0 (R/R_{\text{dec}})^{-3/2}$ at $R > R_{\text{dec}}$. This approximately describes a blast wave decelerating in a uniform medium. The shell is assumed to radiate with bolometric power proportional to the dissipation rate in the blast wave, which gives $\dot{E}(R) = \dot{E}_0 (R/R_{\text{dec}})^2$ at $R < R_{\text{dec}}$ and $\dot{E}(R) = \dot{E}_0 (R/R_{\text{dec}})^{-1}$ at $R > R_{\text{dec}}$. A realistic blast wave has two shocks – forward and reverse – and both can produce a long-lived afterglow. Our toy model may describe the emission from either shock, although it is very much simplified. To illustrate the curvature effect on variability, we add two features: a sudden brief increase in $\dot{E}(R)$ at $R = 3R_{\text{dec}}$ (which simulates a flare) and the abrupt cut-off of $\dot{E}(R)$ at $15R_{\text{dec}}$. For comparison, we show the light curves produced for three cases: isotropic emission in the rest frame of the shell, limb-brightened emission and limb-darkened emission described in Section 4.

(ii) If a relativistic source is limb-darkened, most of its emission in the fixed lab frame is confined within an angle *smaller* than Γ^{-1}. This effect suggests a possible explanation for the lack of jet-break detections in GRBs, as the increased beaming significantly delays the jet break in the observed light curve (Section 3.2). We also discussed in Section 3.3 the consequences of such anisotropy for the apparent size of the radio afterglow source. Although the strong limb darkening appears to be impossible for standard synchrotron afterglows, it may be possible for a different radiative mechanism. For example, limb darkening may be expected for the jitter mechanism (Medvedev & Loeb 1999), as the electrons are preferentially accelerated perpendicular to the shock plane and radiate preferentially in the radial direction.

While this paper was focused on the afterglow, the source of prompt GRB emission may also be intrinsically anisotropic. This may impact models that propose the curvature effect to control the steep X-ray decay at the end of the prompt emission (see e.g. Genet & Granot 2009; Zhang et al. 2009). The effect can be seen in Fig. 4. Anisotropy of the prompt emission may also change the optical depth of the source to high-energy photons, $\tau_{\gamma\gamma}$, as the cross-section for $\gamma\gamma$ reaction strongly depends on the angle between photons. This may affect the constraints on the Lorentz factor of the jet that are inferred from $\tau_{\gamma\gamma} < 1$. The effect is especially strong for emission without front–back symmetry in the source frame; such asymmetric emission would be a more radical assumption compared with the ordinary limb brightening or limb darkening considered in this paper.

REFERENCES

Burrows D. N., Racusin J., 2006, Il Nuovo Cimento B, 121, 1273
Burrows D. N. et al., 2005, Sci, 309, 1833
Chincarini G. et al., 2007, ApJ, 671, 1903
Covino S. et al., 1999, A&A, 348, L1
Frail D. A., 1997, Nat, 389, 261
Genet F., Granot J., 2009, MNRAS, 399, 1328
Genet F., Daigne F., Mochkovitch R., 2007, MNRAS, 381, 732
Granot J., Piran T., Sari R., 1999, ApJ, 527, 236
Grupe D. et al., 2007, ApJ, 662, 443
Hededal C. B., Haugbølle T., Frederiksen J. T., Nordlund Å., 2004, ApJ, 617, L107
Ioka K., Kobayashi S., Zhang B., 2005, ApJ, 631, 429
Kumar P., Panaitescu A., 2000, ApJ, 541, L51
Kumar P., Narayan R., Johnson J. L., 2008, MNRAS, 388, 1729
Lazzati D., Perna R., 2007, MNRAS, 375, L46
Lyutikov M., 2006, MNRAS, 369, L5
Medvedev M. V., Loeb A., 1999, ApJ, 526, 697
Nishikawa K. I. et al., 2009, ApJ, 698, L10
Nousek J. A. et al., 2006, ApJ, 642, 389
Oren Y., Nakar E., Piran T., 2004, MNRAS, 353, L35
Pihlström Y. M., Taylor G. B., Granot J., Doeleman S., 2007, ApJ, 664, 411
Rhoads J., 1997, ApJ 487, L1
Sato G. et al., 2007, ApJ, 657, 359
Schady P. et al., 2007, MNRAS, 380, 1041
Spitkovski A., 2008, ApJ, 682, L5
Taylor G. B., Momjian E., Pihlström Y., Ghosh T., Salter C., 2005, ApJ, 622, 986
Troja E. et al., 2007, ApJ, 665, 599
Uhm Z. L., Beloborodov A. M., 2007, ApJ, 665, L93
Willingale R. et al., 2007, ApJ, 662, 1093
Zhang B., Fan Y. Z., Dyks J., Kobayashi S., Mészáros P., Burrows D. N., Nousek J. A., Gehrels N., 2006, ApJ, 642, 354
Zhang B. B., Zhang B., Liang E.-W., Wang X.-Y., 2009, ApJ, 690, L10

This paper has been typeset from a TEX/LATEX file prepared by the author.